

International Journal of Modern Physics D
 © World Scientific Publishing Company

SCATTERING OF NEUTRINOS BY A ROTATING BLACK HOLE ACCOUNTING FOR THE ELECTROWEAK INTERACTION WITH AN ACCRETION DISK

MAXIM DVORNIKOV

*Pushkov Institute of Terrestrial Magnetism, Ionosphere
 and Radiowave Propagation (IZMIRAN),
 108840 Moscow, Troitsk, Russia
 maxdvo@izmiran.ru*

We study spin effects in the neutrino gravitational scattering by a supermassive black hole with a magnetized accretion disk having a finite thickness. We exactly describe the propagation of ultrarelativistic neutrinos on null geodesics and solve the spin precession equation along each neutrino trajectory. The interaction of neutrinos with the magnetic field is owing to the nonzero diagonal magnetic moment. Additionally, neutrinos interact with plasma of the accretion disk electroweakly within the Fermi approximation. These interactions are obtained to change the polarization of incoming neutrinos, which are left particles. The fluxes of scattered neutrinos, proportional to the survival probability of spin oscillations, are derived for various parameters of the system. In particular, we are focused on the matter influence on the outgoing neutrinos flux. The possibility to observe the predicted effects for astrophysical neutrinos is briefly discussed.

1. Introduction

Neutrino interactions with external fields can significantly modify the dynamics of neutrino oscillations, which were recently confirmed experimentally (see, e.g., Ref. 1). We deal here mainly with neutrino spin oscillations, in which active left handed neutrinos become sterile right particles under the influence of some external fields. Gravitational interaction, in spite of its weakness, can also contribute to neutrino oscillations (see, e.g., Ref. 2).

The propagation of a spinning particle in curved spacetime was first considered in Ref. 3. Then, the quasiclassical approach for the description of the spin evolution of a point-like elementary particle in a gravitational field was formulated in Ref. 4. This method was applied for the studies of neutrino spin oscillations in a curved spacetime both in frames of the General Relativity (GR) in Refs. 5, 6 and in various alternative gravity theories in Refs. 7, 8, 9. The perturbative quantum treatment of neutrino spin oscillations in the gravitational field of a black hole (BH) was carried out in Refs. 10, 11. Quasiclassical and quantum approaches for the studies of spinning particles in a gravitational field were reviewed in Ref. 12.

We considered neutrino spin oscillations in curved spacetimes in Refs. 13, 14, 15, 16, 17, 18, 19. Both stationary^{13–18} and time dependent metrics, like a gravitational

wave,¹⁹ were analyzed. We studied spin effects in the neutrino gravitational scattering by BH in Refs. 15, 16, 17, 18. In a scattering problem, both in- and out-states are in the asymptotically flat spacetime. Thus, we can attribute certain polarization to these states. We studied the cases of both nonrotating and rotating BHs, as well as analyzed the contribution of various external fields to spin oscillations of scattered neutrinos. In the present work, we continue to examine this problem.

The recent observations of the shadows of supermassive BHs (SMBHs) in the centers of M87 and our Galaxy by the Event Horizon Telescope (EHT)^{20,21} were the motivation for the present research. Those results are the unique tests of GR in the strong field limit. There are searches of the high energy neutrinos emission from the centers of some active galaxies.²² If such neutrinos are produced in the vicinity of the SMBH surface, they are strongly lensed analogously to photons observed by the EHT collaboration. External fields, which can exist near SMBHs, will change the neutrino polarization leading to the distortion of the outgoing neutrinos flux. Alternatively, neutrinos emitted in a core-collapsing supernova (SN) explosion can be gravitationally lensed by the SMBH in the center of our Galaxy. Such possibility was discussed in Refs. 23, 24. In this situation, we can also expect the influence of external fields in the curved spacetime on the dynamics of neutrino spin oscillations.

This work is organized in the following way. We start in Sec. 2 with a brief description of the ultrarelativistic neutrinos motion in the Kerr metric. We also describe the neutrino spin evolution in background matter under the influence of electromagnetic and gravitational fields. Then, in Sec. 3, we set up the neutrino interaction with plasma of an accretion disk. The rest of the parameters of the system is chosen in Sec. 4. We present the results for the calculation of the outgoing neutrino fluxes, which account for neutrino spin oscillations, in Sec. 5. The conclusion is given in Sec. 6. We find the component of the four velocity of plasma in the accretion disk in Appendix A. Some computational details are provided in Appendix B.

2. Motion of a neutrino in the Kerr metric and its spin evolution

We study the propagation of a test neutrino in the gravitational field of a rotating BH which is described by the Kerr metric,

$$ds^2 = g_{\mu\nu}dx^\mu dx^\nu = \left(1 - \frac{rr_g}{\Sigma}\right) dt^2 + 2\frac{rr_g a \sin^2 \theta}{\Sigma} dt d\phi - \frac{\Sigma}{\Delta} dr^2 - \Sigma d\theta^2 - \frac{\Xi}{\Sigma} \sin^2 \theta d\phi^2, \quad (2.1)$$

where the Boyer-Lindquist coordinates $x^\mu = (t, r, \theta, \phi)$ are utilized. In Eq. (2.1), we use the following notations:

$$\Delta = r^2 - rr_g + a^2, \quad \Sigma = r^2 + a^2 \cos^2 \theta, \quad \Xi = (r^2 + a^2) \Sigma + rr_g a^2 \sin^2 \theta. \quad (2.2)$$

The mass of BH in Eqs.(2.1) and (2.2) is $M = r_g/2$ and its angular momentum is $J = Ma$, where $0 < a < M$. The BH spin is directed upward from the equatorial plane $\theta = \pi/2$.

The arbitrary motion of a test ultrarelativistic particle in the Kerr metric is characterized by two conserved quantities: the angular momentum L and the Carter

constant Q . If we study the scattering problem, $Q > 0$. The law of motion and the form of a trajectory for such a particle can be found in quadratures. The corresponding quantities are expressed in terms of elliptic integrals. The detailed description of this problem can be found, e.g., in Ref. 25.

If a test particle is spinning, like a neutrino, the invariant equation for the evolution of the particle spin S^μ in a curved spacetime under the influence of the electromagnetic field $F_{\mu\nu}$ and the background matter has the form,¹⁴

$$\frac{DS^\mu}{d\tau} = 2\mu (F^{\mu\nu} S_\nu - U^\mu U_\nu F^{\nu\lambda} S_\lambda) + \sqrt{2} G_F E^{\mu\nu\lambda\rho} G_\nu U_\lambda S_\rho, \quad (2.3)$$

where $U^\mu = \frac{dx^\mu}{d\tau}$ is the four velocity in the world coordinates, τ is the proper time, DS^μ is the covariant differential, $E^{\mu\nu\lambda\rho} = \frac{1}{\sqrt{-g}} \varepsilon^{\mu\nu\lambda\rho}$ is the covariant antisymmetric tensor in a curved spacetime, $g = \det(g_{\mu\nu})$ is the determinant of the metric tensor, μ is the neutrino magnetic moment, $G_F = 1.17 \times 10^{-5} \text{ GeV}^{-2}$ is the Fermi constant, and G_μ is the vector which incorporates the characteristics of the background matter. We discuss its form in details in Sec. 3 below. Although Eq. (2.3) is written down for massive particles, it has the appropriate limit for an ultrarelativistic neutrino. In Eq. (2.3), we suppose that a neutrino is a Dirac particle. Despite some claims about the Majorana nature of neutrinos, this issue is still unresolved.²⁶

It is more convenient to describe the evolution of the neutrino polarization in a locally Minkowskian frame $x_a = e_a^\mu x_\mu$, where e_a^μ are the vierbein vectors which have the form,

$$\begin{aligned} e_0^\mu &= \left(\sqrt{\frac{\Xi}{\Sigma\Delta}}, 0, 0, \frac{arr_g}{\sqrt{\Delta\Sigma\Xi}} \right), \quad e_1^\mu = \left(0, \sqrt{\frac{\Delta}{\Sigma}}, 0, 0 \right), \\ e_2^\mu &= \left(0, 0, \frac{1}{\sqrt{\Sigma}}, 0 \right), \quad e_3^\mu = \left(0, 0, 0, \frac{1}{\sin\theta} \sqrt{\frac{\Sigma}{\Xi}} \right). \end{aligned} \quad (2.4)$$

These vectors diagonalize the metric in Eq. (2.1), $g_{\mu\nu} e_a^\mu e_b^\nu = \eta_{ab}$, where $\eta_{ab} = (1, -1, -1, -1)$ is the Minkowski metric tensor. If we define the three vector of the polarization ζ in the particle rest frame in the locally Minkowskian frame, it obeys the equation,

$$\frac{d\zeta}{dt} = 2(\zeta \times \Omega), \quad \Omega = \Omega_g + \Omega_{\text{em}} + \Omega_{\text{matt}} \quad (2.5)$$

where

$$\begin{aligned} \Omega_g &= \frac{1}{2U^t} \left[\mathbf{b}_g + \frac{1}{1+u^0} (\mathbf{e}_g \times \mathbf{u}) \right], \\ \Omega_{\text{em}} &= \frac{\mu}{U^t} \left[u^0 \mathbf{b} - \frac{\mathbf{u}(\mathbf{u}\mathbf{b})}{1+u^0} + (\mathbf{e} \times \mathbf{u}) \right], \\ \Omega_{\text{matt}} &= \frac{G_F}{\sqrt{2}U^t} \left[\mathbf{u} \left(g^0 - \frac{(\mathbf{g}\mathbf{u})}{1+u^0} \right) - \mathbf{g} \right]. \end{aligned} \quad (2.6)$$

Here $u^a = (u^0, \mathbf{u}) = e_a^\mu U^\mu$, $G_{ab} = (\mathbf{e}_g, \mathbf{b}_g) = \gamma_{abc} u^c$, $\gamma_{abc} = \eta_{ad} e_{\mu;\nu}^d e_b^\mu e_c^\nu$ are the Ricci rotation coefficients, the semicolon stands for the covariant derivative, $f_{ab} =$

4 *Maxim Dvornikov*

$e_a^\mu e_b^\nu F_{\mu\nu} = (\mathbf{e}, \mathbf{b})$ is the electromagnetic field tensor in the locally Minkowskian frame, and $g^a = (g^0, \mathbf{g}) = e^\alpha_\mu G^\mu$. The details of the derivation of Eqs. (2.5) and (2.6) can be found in Ref. 14.

Instead of dealing with Eq. (2.5), we can rewrite it in the form of the effective Schrödinger equation $i\dot{\psi} = H\psi$, where $H = -(\boldsymbol{\sigma}\boldsymbol{\Omega})$ and $\boldsymbol{\sigma}$ are the Pauli matrices. It is more convenient to label a point on a neutrino trajectory with r rather than with t . Thus, we transform the Schrödinger equation to the form,

$$i\frac{d\psi}{dr} = H_r\psi, \quad H_r = -\frac{dt}{dr}\mathcal{U}_2(\boldsymbol{\sigma}\boldsymbol{\Omega})\mathcal{U}_2^\dagger, \quad (2.7)$$

where the matrix $\mathcal{U}_2 = \exp(i\sigma_2\pi/4)$ accounts for the fact that incoming and outgoing neutrinos move oppositely and along the first axis in the locally Minkowskian frame. The derivative dt/dr is taken on the basis of the law of motion of neutrinos; cf., e.g., Refs. 18, 25.

The initial spin wavefunction is $\psi_{-\infty}^T = (1, 0)$. It corresponds to a left polarized neutrino. After reconstructing the neutrino trajectory and solving Eq. (2.7), we get the wave function $\psi_{+\infty}^T = (\psi_{+\infty}^{(R)}, \psi_{+\infty}^{(L)})$ of an outgoing neutrino. The survival probability for a neutrino to remain left polarized after the scattering is $P_{LL} = |\psi_{+\infty}^{(L)}|^2$. Here we account for the fact that the neutrino velocity changes its direction in the locally Minkowskian frame.

3. Neutrino interaction with background matter

In this section, we discuss in details the electroweak interaction of scattering neutrinos with plasma of an accretion disk around BH. The properties of the accretion disk are also considered.

We suppose that the accretion disk consists of the hydrogen plasma. The neutrino interaction with electrons and protons is treated within the Fermi model in the forward scattering approximation. The effective Lagrangian for the interaction of the neutrino bispinor ν with matter has the form,

$$\mathcal{L}_{\text{matt}} = -\frac{G_F}{\sqrt{2}}\bar{\nu}\gamma^\mu(1 - \gamma^5)\nu \cdot G_\mu, \quad (3.1)$$

where γ^μ and γ^5 are the Dirac matrices. The matter characteristics are in the four vector potential G^μ which has the form,¹⁴

$$G^\mu = \sum_{f=e,p} \left(q_f^{(1)} J_f^\mu + q_f^{(2)} \Lambda_f^\mu \right), \quad (3.2)$$

where J_f^μ is the invariant hydrodynamics current of plasma fermions, Λ_f^μ is the plasma invariant polarization, and²⁷

$$q_f^{(1)} = I_{L3}^{(f)} - 2Q_f \sin^2 \theta_W + \delta_{ef}, \quad q_f^{(2)} = -I_{L3}^{(f)} - \delta_{ef}. \quad (3.3)$$

Here $I_{L3}^{(f)}$ is the third component of the weak isospin of background fermions, Q_f is the value of their electric charge, θ_W is the Weinberg angle, $\delta_{ef} = 1$ for electrons and

vanishes for protons. The coefficients $q_f^{(1,2)}$ in Eq. (3.3) correspond to the scattering of electron neutrinos.

The plasma motion in an accretion disk around a rotating BH is quite complex.²⁸ A circular orbit is possible only when an accretion disk is thin and is situated in the BH equatorial plane. Since we study the general gravitational scattering of neutrinos, which involves the neutrino motion both above and below the equatorial plane (see Sec. 4 below), and consider the accretion disk with a nonzero thickness, we assume that plasma in the accretion disk is nonrelativistic and unpolarized. In this case, only $J_f^0 = n_f U_f^t \neq 0$, whereas $J_f^i = 0$ and $\Lambda_f^\mu = 0$. Here n_f is the invariant number density of background fermions, measured by a comoving observer, and U_f^t is the time component of their four velocity. We compute U_f^t in Appendix A; see Eq. (A.4). Eventually, we get that the only nonzero component of G^μ in Eq. (3.2) is $G^t = n_e U_f^t$, where n_e is the electron number density and we suppose that plasma is electroneutral.

Using Eqs. (2.4) and (A.4), we obtain that the vector $g^a = e^a_\mu G^\mu$ has the form,

$$g^a = \frac{n_e U_f^t}{\sqrt{\Xi}} \left(\sqrt{\Sigma \Delta}, 0, 0, -\frac{arr_g \sin \theta}{\sqrt{\Sigma}} \right).$$

The distribution of matter in an accretion disk is quite model dependent. We suppose that²⁹

$$n_e(r, \theta) = n_e^{(c)} \exp \left(-\frac{r^2 \cos^2 \theta}{2H^2} \right), \quad (3.4)$$

where H is the disk thickness and $n_e^{(c)}$ is the central density, i.e. the density at the equatorial plane. We take that³⁰ $n_e^{(c)}(r) \propto n_0 r^{-3/2}$, where $n_0 = 10^{18} \text{ cm}^{-3}$ for SMBH with $M = 10^8 M_\odot$.³¹

The matter contribution to the vector Ω , which determines the spin precession of ultrarelativistic neutrinos in Eq. (2.6), takes the form,

$$\Omega_{\text{matt}} = \frac{G_F}{\sqrt{2}U^t} \mathbf{u} \left(g^0 - \frac{(\mathbf{g}\mathbf{u})}{1+u^0} \right), \quad (3.5)$$

where we neglect the term $\propto \mathbf{g}/U^t$ for ultrarelativistic neutrinos. Nevertheless both \mathbf{u}/U^t and $\mathbf{u}/(1+u^0)$ are finite in Eq. (3.5).

4. Parameters of the system

We study the gravitational scattering of ultrarelativistic neutrinos by a rotating SMBH surrounded with a magnetized accretion disk with a finite thickness. The incoming flux of neutrinos is parallel to the equatorial plane of BH. Nevertheless, unlike Refs. 15, 16, 17, we do not restrict ourselves by the equatorial neutrino motion. Incoming neutrinos are emitted from the direction $(\theta, \phi)_s = (\pi/2, 0)$. A remote neutrino detector is in the arbitrary position with the angular coordinates $(\theta_{\text{obs}}, \phi_{\text{obs}})$.

The mass of SMBH is taken to be $10^8 M_\odot$. The accretion disk around this SMBH consists of hydrogen plasma with the electron density distribution in Eq. (3.4) (see also Refs. 29, 31). The main uncertainty among the disk parameters is its thickness H . We vary it in the range $(1 - 10)r_g$ in our simulations (see, e.g., Ref. 32), considering disks with a nonzero thickness. We study the simplified model of the accretion disk which does not account for the disk rotation. The neutrino interaction with plasma is within the Fermi approximation of the standard model. We consider only the forward scattering of electron neutrinos on plasma fermions.

We take into account the poloidal component of the magnetic field which is based on the following vector potential in the world coordinates:³³

$$A_t = Ba \left[1 - \frac{rr_g}{2\Sigma}(1 + \cos^2 \theta) \right], \quad A_\phi = -\frac{B}{2} \left[r^2 + a^2 - \frac{a^2 rr_g}{\Sigma}(1 + \cos^2 \theta) \right] \sin^2 \theta, \quad (4.1)$$

where the amplitude B is supposed to scale with radius as $B \propto B_0 r^{-5/4}$.³⁴ The strength B_0 , which is the magnetic field at the inner radius of the disk, is taken to be $B_0 = 3.2 \times 10^2$ G. This value of B_0 is below the Eddington limit for $M = 10^8 M_\odot$.³⁵ The toroidal magnetic field, which is inevitably generated in a thick disk and can be rather strong, is not considered in our model. We plan to account for both the realistic plasma motion and the toroidal magnetic field in one of the forthcoming works.

A neutrino is taken to be a Dirac particle with a nonzero magnetic moment μ . We consider the values of μ in the range $\mu = (10^{-14} - 10^{-13})\mu_B$. Such magnetic moments are within the theoretical and astrophysical constraints on neutrino magnetic moments established in Refs. 36, 37.

To reconstruct the neutrino motion, first, we find the $\theta(r)$ dependence. One can find the details of this procedure in Refs. 18, 25. The knowledge of $\phi(r)$ is not necessary since the spin evolution does not depend on ϕ . We just need to obtain the final scattering angle ϕ_{obs} . This fact significantly accelerates numerical simulations allowing us to involve more test particles and perform more frequent meshing in the radial direction. Now we use 2500 test neutrinos in the incoming flux. However, some of these particles are not involved in the scattering since they fall to the BH shadow region.

The right hand side of Eq. (2.7) is given only in the discrete nodes r_i . Moreover, the grid r_i is irregular. Thus, we apply the two-step Adams–Bashforth method for the numerical integration of Eq. (2.7). The corresponding iterative procedure is provided in Appendix B; see Eqs. (B.4) and (B.5). It allows us to increase the accuracy of numerical simulations compared to Ref. 18 where the Euler method was used.

5. Results

In this section we present the results of the numerical solution of Eq. (2.7) accounting for the values of the parameters in Sec. 4.

Ultrarelativistic neutrinos are emitted as left polarized particles in frames of the standard model. A terrestrial neutrino telescope can detect only left neutrinos as well. Thus, if $F_0 \propto d\sigma/d\Omega$ is the flux of scalar test particles, the observed flux of neutrinos is $F_\nu = P_{LL}F_0$. Here $d\sigma/d\Omega$ is the differential cross section of the gravitational scattering. Our main goal is to find the ratio F_ν/F_0 for neutrinos gravitationally scattered by BH and to account for the neutrino spin precession in all external fields. We normalize the neutrino flux by F_0 in order to avoid the singularities in the cross section which are inherent in the gravitational scattering of both spinning and spinless particles.³⁸ The detailed study of the gravitational scattering of scalar test particles off a rotating BH can be found in Ref. 39. We utilize the term ‘scalar particles’ meaning their motion along null geodesics.

In the present work, we use the modified method for the integration of Eq. (2.7); cf. Appendix B. We should check the behavior of the solution when only the gravitational interaction is taken into account. We expect that $F_\nu/F_0 \approx 1$, i.e. no spin oscillations occur in a purely gravitational scattering. The corresponding general theorem has been proven in Ref. 18. We show $F_\nu/F_0 = P_{LL}$ in Fig. 1 for BHs with different angular momenta.

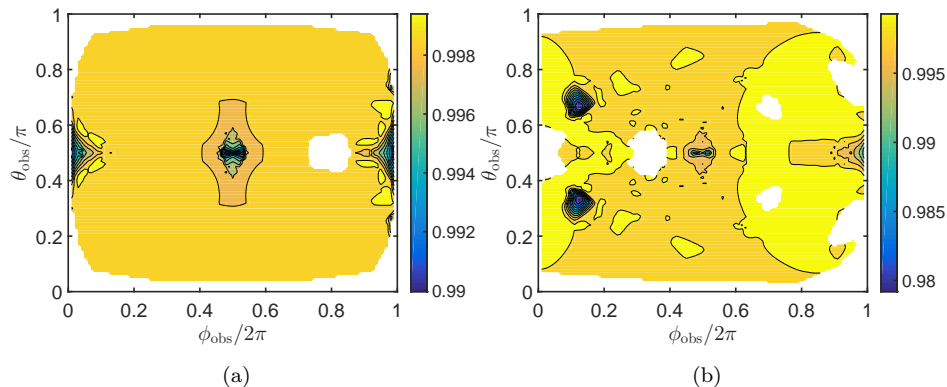


Fig. 1. The ratio of the fluxes of spinning ultrarelativistic neutrinos F_ν and the scalar particles F_0 scattered off BH with different spins when only the gravitational interaction is accounted for. Panel (a): $a = 0.02M$; panel (b): $a = 0.98M$.

One can see in Fig. 1 that the deviation of F_ν/F_0 from one is less than 1% for the majority of $(\theta_{\text{obs}}, \phi_{\text{obs}})$. The higher accuracy of simulations compared to that in Ref. 18 is owing to the two-step Adams–Bashforth method represented in Appendix B. The result that $F_\nu/F_0 \approx 1$ means that our simulations are reliable.

One has white areas Fig. 1 (see also Figs. 2 and 3 below), which are present because of the insufficient number of neutrinos scatter to these regions. Thus, 2D cubic interpolation, used in our simulations, is unable to create contour plots there. This shortcoming may be eliminated by a significant enhancement of the test particles

number. We plan to implement this task in a future work.

Now, we add the neutrino interaction with the magnetic field and the accretion disk to Eq. (2.7). First, we consider an almost nonrotating SMBH with $a = 0.02M$. We show the ratio F_ν/F_0 in Fig. 2. We plot F_ν/F_0 in case when the magnetic interaction is dominant, i.e. $V_m = 0$, in Fig. 2(a) for $\mu = 10^{-14}\mu_B$ and in Fig. 2(b) for $\mu = 10^{-13}\mu_B$. In both cases, $B_0 = 3.2 \times 10^2$ G. Then, in Figs. 2(c)-2(f), we account for a nonzero interaction with background matter by setting the electron number density near the SMBH surface to $n_0 = 10^{18} \text{ cm}^{-3}$. Figures 2(c) and 2(d) correspond to the disk thickness $H = r_g$, whereas Figs. 2(e) and 2(f) to $H = 10r_g$.

We can see in Figs. 2(c) and 2(d) that the neutrino interaction with plasma of the accretion disk suppresses neutrino spin oscillations. We remind that spin oscillations of neutrinos are in the resonance when only the magnetic interaction is taken into account (see, e.g., Ref. 40, where this problem is discussed in the flat spacetime). The electroweak interaction with matter shifts spin oscillations out of the resonance. It explains the behavior of P_{LL} in Figs. 2(c) and 2(d). Moreover, the consideration of a thicker disk in Figs. 2(e) and 2(f) results in the further enhancement of the survival probability since the regions with the great P_{LL} become wider. This result is explained by the fact that more scattered neutrinos interact with matter if the disk is thicker.

Finally, we plot F_ν/F_0 in Fig. 3 for an almost maximally rotating SMBH with $a = 0.98M$. Qualitatively, the behavior of the survival probability resembles that in Fig. 2, which is discussed above. We just mention that the interaction with matter is more pronounced for a small neutrino magnetic moment. Indeed, one can see in Figs. 3(c) and 3(e) that neutrino spin oscillations are almost suppressed.

6. Conclusion

In the present work, we have studied the scattering of ultrarelativistic neutrinos off a rotating SMBH surrounded by a magnetized accretion disk with a nonzero thickness. The flux of left polarized incoming neutrinos was taken to propagate parallel to the equatorial plane of BH. However, we did not restrict ourselves to a purely equatorial neutrino motion. These neutrinos have been strongly gravitationally lensed towards a distant observer with the arbitrary angular coordinates $0 < \theta_{\text{obs}} < \pi$ and $0 < \phi_{\text{obs}} < 2\pi$.

Unlike scalar particles or photons, the polarization of neutrinos is important for their detection since we cannot observe sterile right neutrinos. That is why, besides the reconstruction of the particle trajectories in the curved spacetime, we had to study neutrino spin precession in the external fields. We have supposed that a neutrino is a Dirac particle having a nonzero magnetic moment, which provides the interaction with a poloidal magnetic field in the accretion disk. The neutrino electroweak interaction with plasma in the disk is considered in frames of the Fermi approximation.

In Sec. 2, we have outlined the neutrino motion in the Kerr metric and the

description of the spin evolution in external fields in curved spacetime. The neutrino interaction with background matter and the model of the accretion disk have been described in Sec. 3. The characteristics of the magnetic field are the same as in Ref. 18. Therefore we did not discuss them in details here. Then, in Sec. 4, we have specified the rest of the parameters in the system and considered some details of the numerical simulations.

We have presented our results in Sec. 5. The fluxes of spinning neutrinos have been found for various parameters of the system. We have confirmed the general theorem, proven in Ref. 18, that the polarization of ultrarelativistic neutrinos is unchanged in a purely gravitational scattering. Then, we have obtained that the neutrino interaction with plasma of an accretion disk suppresses neutrino spin oscillations. This feature, known in flat spacetime, has been demonstrated for the neutrino gravitational scattering. Besides the consideration of the accretion disk with a finite thickness, one of the advantages of the present work, compared to Ref. 18, was the more precise numerical integration of Eq. (2.7). It allowed us to significantly increase the accuracy of the simulations.

The derivation of the time component of the four velocity of matter in the accretion disk has been provided in Appendix A. In Appendix B, we have described the more precise method of the integration of Eq. (2.7) in a nonuniform grid.

The results obtained allow one to explore the characteristics of inner parts of the accretion disk around SMBH in our Galaxy, e.g., with neutrinos emitted in a SN explosion. The huge number of such neutrinos are expected to be observed with the existing or future neutrino telescopes. If such neutrinos are gravitationally lensed by the central SMBH, we have to account for the interaction with strong external fields in curved spacetime near this SMBH.

Appendix A. Derivation of U^t for an arbitrary position of a plasma particle

The action for a test particle moving in the Kerr metric has the form, $S = -Et + L\phi + \dots$, where we show only the terms responsible for the conserved energy, E , and the projection of the particle angular momentum on the BH spin, L . The canonical four momentum of a massive particle reads $p_\mu = mU_\mu = -\partial_\mu S$. Thus, we have that

$$m(g_{tt}U^t + g_{t\phi}U^\phi) = E, \quad m(g_{\phi t}U^t + g_{\phi\phi}U^\phi) = -L. \quad (\text{A.1})$$

Solving Eq. (A.1), we get that⁴¹

$$U^t = -\frac{(Eg_{\phi\phi} + Lg_{\phi t})}{m(g_{\phi t}^2 - g_{\phi\phi}g_{tt})}. \quad (\text{A.2})$$

Using the Kerr metric components in Eq. (2.1), one rewrites Eq. (A.2) in the form,

$$U^t = \frac{E[(r^2 + a^2)\Sigma + rr_g a^2 \sin^2 \theta] - Lrr_g a \sin^2 \theta}{m\Sigma\Delta \sin^2 \theta}. \quad (\text{A.3})$$

10 *Maxim Dvornikov*

If a particle moves in the equatorial plane with $\theta = \pi/2$, we reproduce the expression for U^t obtained in Ref. 16.

Finally, if a particle is nonrelativistic, it has $E = m$ and $L = 0$. We obtain, basing on Eq. (A.3), that

$$U^t = \frac{\Xi}{\Sigma \Delta \sin^2 \theta}, \quad (\text{A.4})$$

which is used in Sec. 3 as U_f^t .

Appendix B. Two-step Adams–Bashforth method for an irregular grid

We discuss the solution of the single first order differential equation

$$y' = f(x, y). \quad (\text{B.1})$$

The generalization of the results to a system of equations is straightforward. If the function $f(x, y)$ in Eq. (B.1) is given only in discrete points f_i , we cannot use the precise Runge-Kutta method.

The value of the function at the $(i + 2)$ th node is

$$y_{i+2} = y_{i+1} + \int_{x_{i+1}}^{x_{i+2}} f(x, y(x)) dx. \quad (\text{B.2})$$

We replace the integrand in Eq. (B.2) with the linear polynomial

$$f(x, y(x)) \rightarrow p(x) = \frac{x - x_i}{x_{i+1} - x_i} f_{i+1} + \frac{x - x_{i+1}}{x_i - x_{i+1}} f_i. \quad (\text{B.3})$$

One can see that $p(x_i) = f_i$ and $p(x_{i+1}) = f_{i+1}$.

Integrating in Eq. (B.2) and accounting for Eq. (B.3), we get that

$$y_{i+2} = y_{i+1} + C_1 f_{i+1} + C_0 f_i, \quad (\text{B.4})$$

where

$$C_1 = \frac{(x_{i+2} - x_{i+1})}{2(x_{i+1} - x_i)}(x_{i+2} + x_{i+1} - 2x_i), \quad C_0 = \frac{(x_{i+2} - x_{i+1})}{2(x_{i+1} - x_i)}(x_{i+1} - x_{i+2}). \quad (\text{B.5})$$

If the grid is regular with the step h , we obtain in Eq. (B.5) that $C_1 = \frac{3}{2}h$ and $C_0 = -\frac{1}{2}h$. It reproduces the result known previously (see, e.g., Ref. 42).

Equations (B.4) and (B.5) are more precise than the Euler method. We use them in Sec. 5 to solve Eq. (2.7), where the grid is irregular.

References

1. F. P. An, et al. (Daya Bay collaboration), arXiv:2211.14988.
2. D. Píríz, M. Roy, and J. Wudka, *Phys. Rev. D* **54** (1996) 1587, hep-ph/9604403.
3. A. Papapetrou, *Proc. Roy. Soc. Lond. A* **209** (1951) 248.
4. A. A. Pomeranskiĭ and I. B. Khriplovich, *J. Exp. Theor. Phys.* **86** (1998) 839, gr-qc/9710098.

5. S. A. Alavi and S. Nodeh, *Grav. Cosmol.* **19** (2013) 129, arXiv:1108.3593.
6. G. Baym and J.-C. Peng, *Phys. Rev. D* **103** (2021) 123019, arXiv:2103.11209.
7. S. A. Alavi and S. Nodeh, *Phys. Scr.* **90** (2015) 035301, arXiv:1301.5977.
8. S. Chakraborty, *J. Cosmol. Astropart. Phys.* **10** (2015) 019, arXiv:1506.02647.
9. L. Mastrototaro and G. Lambiase, *Phys. Rev. D* **104** (2021) 024021, arXiv:2106.07665.
10. F. Sorge and S. Zilio, *Class. Quantum Grav.* **24** (2007) 2653.
11. F. Sorge, *Class. Quantum Grav.* **29** (2012) 045002.
12. S. N. Vergeles, N. N. Nikolaev, Yu. N. Obukhov, A. Ya. Silenko, and O. V. Teryaev, *Phys.—Usp.* **66** (2) (2023), arXiv:2204.00427.
13. M. Dvornikov, *Int. J. Mod. Phys. D* **15** (2006) 1017, hep-ph/0601095.
14. M. Dvornikov, *J. Cosmol. Astropart. Phys.* **06** (2013) 015 arXiv:1306.2659.
15. M. Dvornikov, *Phys. Rev. D* **101** (2020) 056018, arXiv:1911.08317.
16. M. Dvornikov, *Eur. Phys. J. C* **80** (2020) 474, arXiv:2006.01636.
17. M. Dvornikov, *J. Cosmol. Astropart. Phys.* **04** (2021) 005, arXiv:2102.00806.
18. M. Dvornikov, *Class. Quantum Grav.* **40** (2023) 015002, arXiv:2206.00042.
19. M. Dvornikov, *Phys. Rev. D* **99** (2019) 116021, arXiv:1902.11285.
20. K. Akiyama et al. (Event Horizon Telescope Collaboration), *Astrophys. J. Lett.* **875** (2019) L1, arXiv:1906.11238.
21. K. Akiyama et al. (Event Horizon Telescope Collaboration), *Astrophys. J. Lett.* **930** (2022) L12.
22. R. Abbasi et al. (IceCube Collaboration), *Phys. Rev. D* **106** (2022) 022005, arXiv:2111.10169.
23. O. Mena, I. Mocioiu, and C. Quigg, *Astropart. Phys.* **28** (2007) 348, astro-ph/0610918.
24. J. M. LoSecco, *Universe* **7** (2021) 335, arXiv:2109.01957.
25. S. Chandrasekhar, *The mathematical theory of black holes* (Clarendon Press, Oxford, 1983).
26. S. M. Bilenky, *Universe* **6** (2020) 134, arXiv:2008.02110.
27. M. Dvornikov and A. Studenikin, *J. High Energy Phys.* **09** (2002) 016, hep-ph/0202113.
28. M. A. Abramowicz and P. C. Fragile, *Living Rev. Relativ.* **16** (2013) 1, arXiv:1104.5499.
29. R. Stehle and H. C. Spruit, *Mon. Not. R. Astron. Soc.* **304** (1999) 674.
30. R. Narayan and I. Yi, *Astrophys. J. Lett.* **428** (1994) L13, astro-ph/9403052.
31. J. Jiang, A. C. Fabian, T. Dauser, L. Gallo, J. A. Garcia, E. Kara, M. L. Parker, J. A. Tomsick, D. J. Walton, and C. S. Reynolds, *Mon. Not. R. Astron. Soc.* **489** (2019) 3436, arXiv:1908.07272.
32. A. Sądowski, *Astrophys. J. Suppl.* **183** (2009) 171, arXiv:0906.0355.
33. R. M. Wald, *Phys. Rev. D* **10** (1974) 1680.
34. R. D. Blandford and D. G. Payne, *Mon. Not. R. Astron. Soc.* **199** (1982) 883.
35. V. S. Beskin, *MHD Flows in Compact Astrophysical Objects: Accretion, Winds and Jets* (Springer, Heidelberg, 2010).
36. N. F. Bell, V. Cirigliano, M. J. Ramsey-Musolf, P. Vogel, and M. B. Wise, *Phys. Rev. Lett.* **95** (2005) 151802, hep-ph/0504134.
37. N. Viaux, M. Catelan, P. B. Stetson, G. G. Raffelt, J. Redondo, A. A. R. Valcarce, and A. Weiss, *Astron. Astrophys.* **558** (2013) A12, arXiv:1308.4627.
38. S. K. Bose and M. Y. Wang, *J. Math. Phys.* **15** (1974) 957.
39. V. Bozza, *Phys. Rev. D* **78** (2008) 063014, arXiv:0806.4102.
40. M. B. Voloshin, M. I. Vysotskiĭ, and L. B. Okun', *Sov. Phys. JETP* **64** (1986) 446,
41. C. M. Will, *Class. Quantum Grav.* **29** (2012) 217001, arXiv:1208.3931.
42. G. A. Korn and T. M. Korn, *Mathematical Handbook for Scientists and Engineers:*

12 *Maxim Dvornikov*

Definitions, Theorems and Formulas for Reference and Review (McGraw-Hill, New York, 1968), 2nd ed.

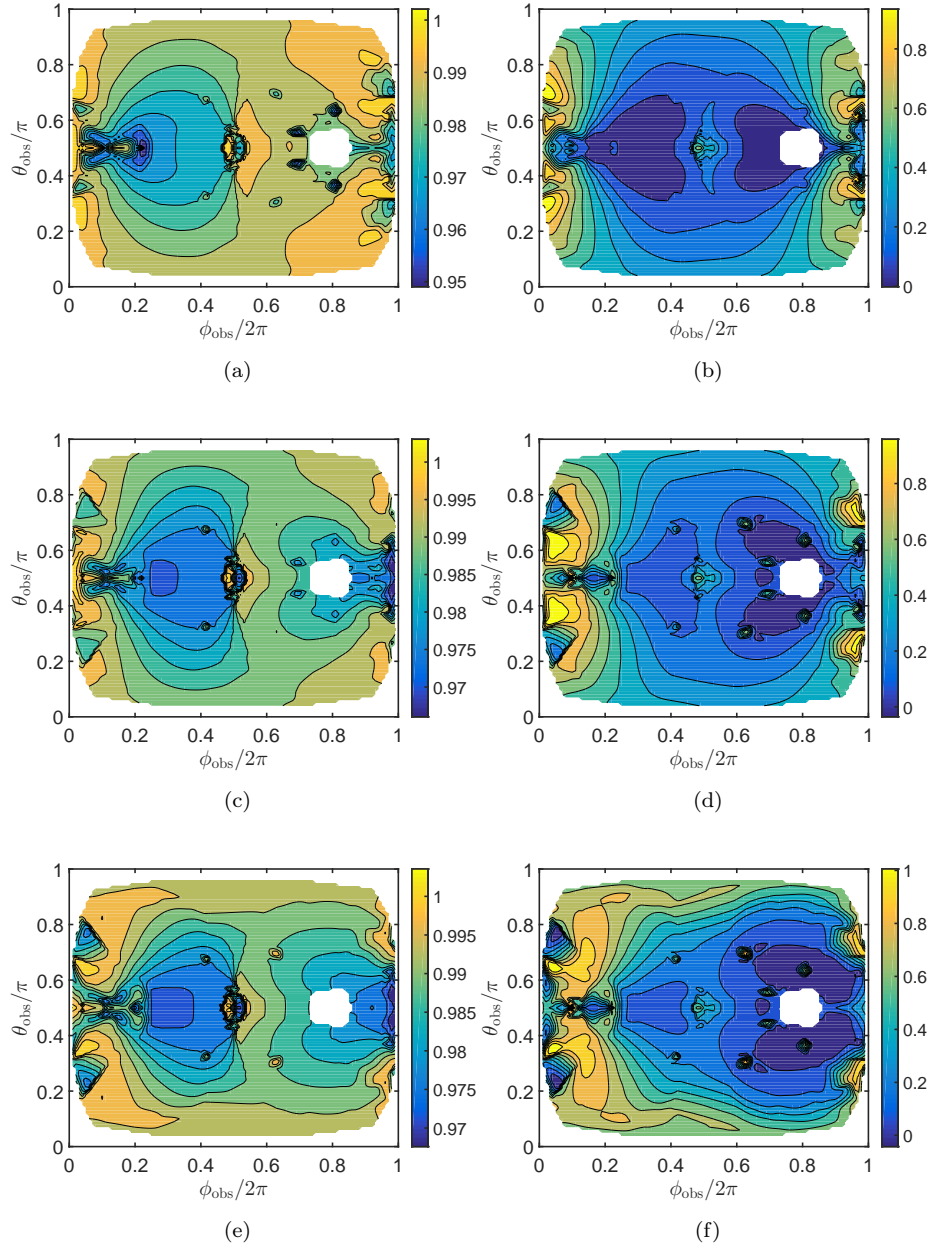


Fig. 2. The ratio of the fluxes F_ν/F_0 for ultrarelativistic ν_e scattered off the almost nonrotating SMBH with $a = 0.02M$ and $M = 10^8 M_\odot$. Panel (a): $V_B = \mu B_0 r_g = 2.7 \times 10^{-2}$, $V_m = G_F n_0 r_g / \sqrt{2} = 0$. Panel (b): $V_B = 2.7 \times 10^{-1}$, $V_m = 0$. Panel (c): $V_B = 2.7 \times 10^{-2}$, $V_m = 10^{-1}$, $H = r_g$. Panel (d): $V_B = 2.7 \times 10^{-1}$, $V_m = 10^{-1}$, $H = r_g$. Panel (e): $V_B = 2.7 \times 10^{-2}$, $V_m = 10^{-1}$, $H = 10r_g$. Panel (f): $V_B = 2.7 \times 10^{-1}$, $V_m = 10^{-1}$, $H = 10r_g$.

14 *Maxim Dvornikov*

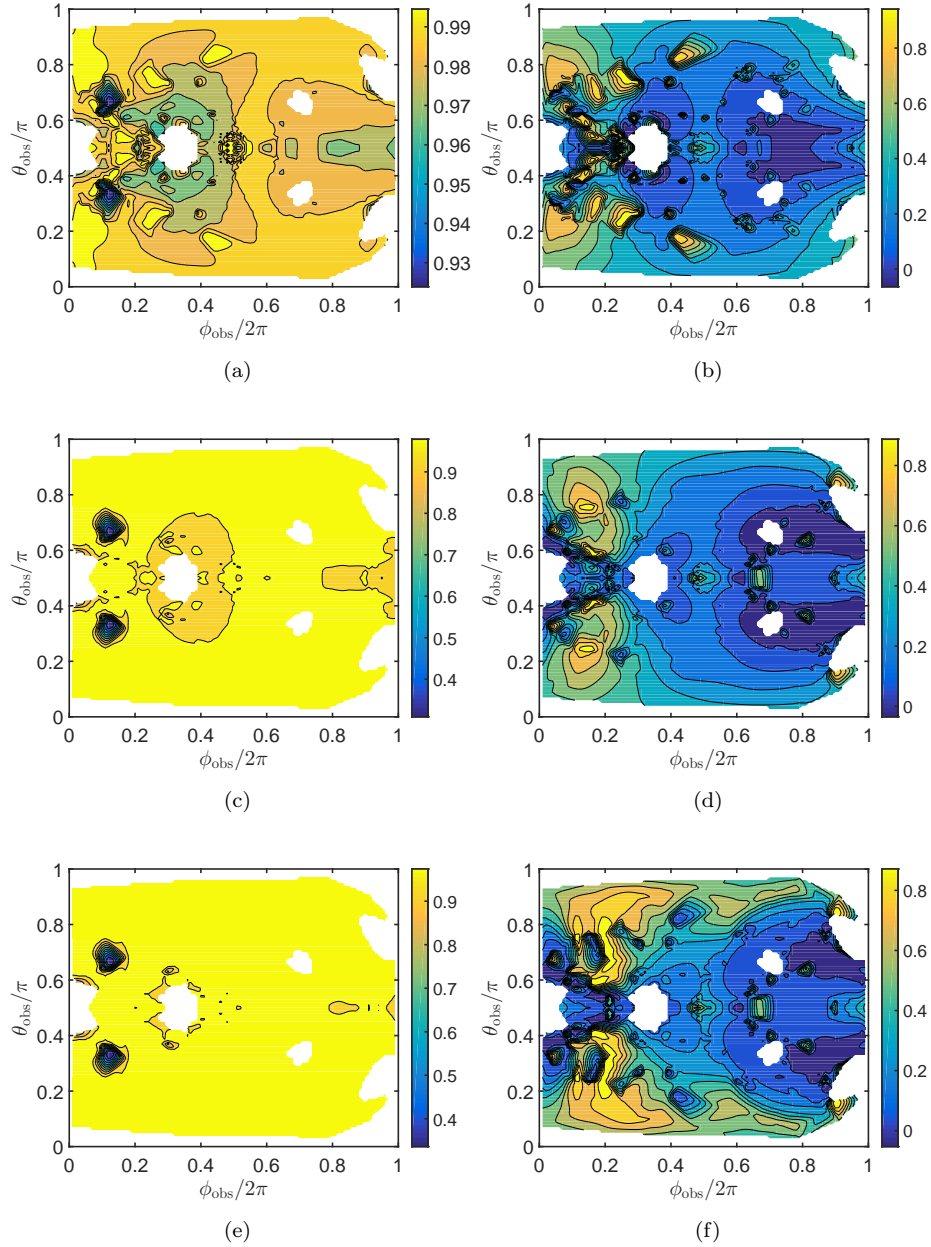


Fig. 3. The same as in Fig. 2 for $a = 0.98M$, i.e. SMBH is almost maximally rotating.